

Coastal sea level rise with warming above 2 °C

Svetlana Jevrejeva^{a,1}, Luke P. Jackson^{a,b}, Riccardo E. M. Riva^{c,d}, Aslak Grinsted^e, and John C. Moore^{f,g,1}

^aNational Oceanography Centre, Liverpool L3 5DA, United Kingdom; ^bProgramme for Economic Modelling, Nuffield College, University of Oxford, Oxford OX1 1NF, United Kingdom; ^cDepartment Geoscience and Remote Sensing, Delft University of Technology, 2628CN Delft, The Netherlands; ^dClimate Institute, Delft University of Technology, 2628CN Delft, The Netherlands; ^eCentre for Ice and Climate, Niels Bohr Institute, University of Copenhagen, DK-2100 Copenhagen, Denmark; ^fJoint Center for Global Change Studies, College of Global Change and Earth System Science, Beijing Normal University, Beijing 100875, China; and ^gArctic Centre, University of Lapland, FI-96101 Rovaniemi, Finland

Edited by Anny Cazenave, Centre National d'Etudes Spatiales, Toulouse, France, and approved October 3, 2016 (received for review April 1, 2016)

Two degrees of global warming above the preindustrial level is widely suggested as an appropriate threshold beyond which climate change risks become unacceptably high. This “2 °C” threshold is likely to be reached between 2040 and 2050 for both Representative Concentration Pathway (RCP) 8.5 and 4.5. Resulting sea level rises will not be globally uniform, due to ocean dynamical processes and changes in gravity associated with water mass redistribution. Here we provide probabilistic sea level rise projections for the global coastline with warming above the 2 °C goal. By 2040, with a 2 °C warming under the RCP8.5 scenario, more than 90% of coastal areas will experience sea level rise exceeding the global estimate of 0.2 m, with up to 0.4 m expected along the Atlantic coast of North America and Norway. With a 5 °C rise by 2100, sea level will rise rapidly, reaching 0.9 m (median), and 80% of the coastline will exceed the global sea level rise at the 95th percentile upper limit of 1.8 m. Under RCP8.5, by 2100, New York may expect rises of 1.09 m, Guangzhou may expect rises of 0.91 m, and Lagos may expect rises of 0.90 m, with the 95th percentile upper limit of 2.24 m, 1.93 m, and 1.92 m, respectively. The coastal communities of rapidly expanding cities in the developing world, and vulnerable tropical coastal ecosystems, will have a very limited time after midcentury to adapt to sea level rises unprecedented since the dawn of the Bronze Age.

2° warming | coastal sea level rise | probabilistic sea level projections | regional sea level rise

The threshold for dangerous climate change is widely reported to be about 2 °C above preindustrial temperature; therefore, international efforts have been generally aimed at keeping average global temperatures below this (1, 2). Fragile coastal ecosystems (3) and increasing concentrations of population and economic activity in maritime cities (4) are reasons why future sea level rise is one of the most damaging aspects of the warming climate (5). Furthermore, sea level is set to continue to rise for centuries after greenhouse gas emissions concentrations are stabilized due to system inertia and feedback time scales (5–7). Impact, risk, adaptation policies, and long-term decision-making in coastal areas depend on regional and local sea level rise projections, and local projections can differ substantially from the global one (6, 8–11). Coastal sea level projections should also take into account the local vertical land movement that is caused both by glacial isostatic adjustments (GIAs) due to redistribution of masses subsequent to the end of the last ice age (12–14), and subsidence due to groundwater extraction, urbanization, tectonics, and river delta sedimentation rates (15).

Global sea level is an integrated climate system response to changes in radiative forcing that alters the dynamics and thermodynamics of the atmosphere, ocean, and cryosphere. In a warming climate, global sea level will rise due to melting of land-based glaciers and ice sheets and from the thermal expansion of ocean waters. Sea level rise along coastlines displays complex spatial patterns (8–10) due to the dynamic redistribution of ocean mass (11–14) and the gravitational effects of ice sheets and glaciers melting into the ocean, so-called “fingerprints” (12), associated with specific geographical distributions of ice loss from mountain glaciers, Greenland, and Antarctica ice sheets and due to changes in man-made reservoirs and groundwater extraction (6).

Projections of each sea level component are characterized by uncertainties (6, 16), the largest due to limitations of process-based models to simulate the dynamics of ice mass loss from the Greenland and Antarctica ice sheets (6, 17, 18). This lack of precise knowledge can be accommodated in a probabilistic approach (9, 10, 16) where the sea level rise for each component is represented by continuous probability density functions (pdfs). Future sea level has been previously expressed in terms of levels at specific dates under a climate scenario accounting for uncertainties in the response of the sea level contributors for Northern Europe by 2100 (10) and for individual tide gauge stations through to 2200 (9). However, here we introduce pdfs for each individual component of sea level rise and global sea level rise under warming of 2 °C, 4 °C, or 5 °C (Fig. 1 C–H and *Materials and Methods*). We calculated spatial patterns of dynamic changes in sea surface height and global average steric sea level change from 33 models involving 83 realizations, in the Coupled Model Intercomparison Project Phase 5 (CMIP5) (Table S1 and Fig. S1 A–C). Spatial patterns of ice loss from glaciers and ice sheets (Fig. S1 D–F) are derived from present-day spatial attribution of terrestrial ice loss (14) and scaled using the pdfs of contributions from glaciers and ice sheets with warming of 2 °C, 4 °C, or 5 °C (Fig. 1 C, E, and G). The land water fingerprint is calculated using projected changes in land water storage (19). At each point on the global ocean, a putative sea level can be generated by random sampling of the component pdfs and summing. Repeating this process 5,000 times provides enough realizations of sea level to create the pdf for sea level rise at each point on the globe. Finally, to account for the redistribution of ocean mass due to GIA, we add the time-integrated global sea level field from the ICE-6G C (VM5a) model (13) to the sum of sea level components. Here we do not take into account the local vertical land movement caused by subsidence due to groundwater

Significance

Warming of 2 °C will lead to an average global ocean rise of 20 cm, but more than 90% of coastal areas will experience greater rises. If warming continues above 2 °C, then, by 2100, sea level will be rising faster than at any time during human civilization, and 80% of the global coastline is expected to exceed the 95th percentile upper limit of 1.8 m for mean global ocean sea level rise. Coastal communities, notably rapidly expanding cities in the developing world; small island states; United Nations Educational, Scientific and Cultural Organization Cultural World Heritage sites; and vulnerable tropical coastal ecosystems will have a very limited time after midcentury to adapt to these rises.

Author contributions: S.J. designed research; L.P.J. performed research; R.E.M.R. and A.G. contributed new reagents/analytic tools; S.J. and L.P.J. analyzed data; and S.J., L.P.J., R.E.M.R., A.G., and J.C.M. wrote the paper.

The authors declare no conflict of interest.

This article is a PNAS Direct Submission.

¹To whom correspondence may be addressed. Email: sveta@noc.ac.uk or john.moore.bnu@gmail.com.

This article contains supporting information online at www.pnas.org/lookup/suppl/doi:10.1073/pnas.1605312113/-DCSupplemental.

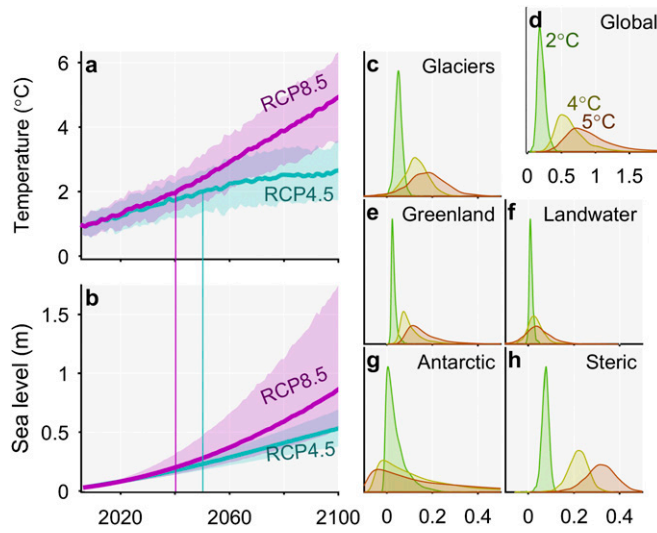


Fig. 1. Projections (5%, 50%, and 95% quantiles) of (A) global average surface temperature and (B) global sea level rise since 2005, with dates when expected global mean temperature rises 2 °C. (C–H) The sea level pdfs for the individual components, and for combined global sea level rise for warmings of 2 (green), 4 (yellow) and 5 °C (brown): (C) glaciers, (D) global, (E) Greenland, (F) land water, (G) Antarctic, and (H) steric. The x axis is sea level (meters) and y axis is probability density.

extraction, urbanization, and river delta sedimentation due to the general lack of long-term projections for global coastlines and individual cities (15). However, for some cities, including Manila, Jakarta, Bangkok, Ho Chi Minh City, and New Orleans, subsidence estimates do exist (15), and we discuss their sea level projections and the large uncertainties associated with local vertical land movement.

Results

With the Representative Concentration Pathway 8.5 (RCP8.5) emission scenario, a 2 °C warming relative to the preindustrial period is expected by 2041 (Fig. 1A), reaching 4 °C by 2083, continuing to a median projected warming of almost 5 °C by 2100 (6, 20), with consequent global mean sea level rises (Fig. 1B). By 2040, the median rate of sea level rise is expected to be 6 mm·y⁻¹, 3 times larger than the rate of sea level rise during the 20th century. If RCP8.5 is followed, then, in contrast to the almost 200-y (1850–2040) period taken to raise mean global temperatures by 2 °C, a further rise of 2 °C occurs in the following 43 y to 2083 (Table 1). This rate of change would probably be unprecedented over the Holocene, and certainly within the period of large human settlements; sea level will continue to rise, with 0.9 m expected by 2100, with 95th percentile upper limit of 1.8 m (10, 16).

Table 1. Probabilistic projections of global sea level rise with global average surface temperature of 2 °C and 4 °C and by the end of the 21st century under the RCP8.5 scenario

Global warming °C	Year	Global sea level rise, m		Rate of global sea level rise, mm·y ⁻¹	
		Median	5 to 95%	Median	5 to 95%
2	2041	0.22	0.15–0.33	6	4–8
4	2083	0.63	0.39–1.24	10	7–28
5*	2100	0.86	0.53–1.78	14	7–35

*Some models suggest warming of 5 °C by 2100 (20).

Fig. 2A shows that, with 2 °C warming, more than 70% of global coastlines will experience sea level rise exceeding the median global rise of 0.2 m, with ratio up to 1.5 of local sea level to global sea level rise along the Atlantic coast of North America and Norway (Fig. 3A). A 95th percentile upper limit exceeding 0.3 m is projected for most coastlines (Fig. 2B), including the extensive, low-lying coastal regions in South and Southeast Asia, which are often located along deltaic systems vulnerable to storm surges (3). By 2030, when coastal sea level rises of up to 0.3 m are expected under most RCP scenarios, there will be a population of 400 million living in 23 coastal megacities, including 370 million living on the coasts of Asia, Africa, and South America (21). Projected land subsidence rates in coastal cities, mainly due to excessive groundwater extraction, are comparable to, or exceed, expected rates of sea level rises, resulting in an additional 0.2 m sea level rise in Bangkok and Ho Chi Minh City and 1.8 m in Jakarta by 2025 (15, 19). Each of these cities will house more than 10 million inhabitants by 2030.

If global temperatures reach 4 °C (by 2083 under RCP8.5), then more than 80% of coastlines will exceed the global median sea level rise of 0.6 m (Fig. 2C), with a 95th percentile rise of 1.3 m (Fig. 2D). Under RCP8.5, by the end of 21st century, the expected mean sea level rise will be 0.9 m, with 95th percentile upper limit above 1.8 m (Fig. 2E and F). The highest sea level rises, exceeding 2.0 m (Fig. 2F), are projected for the small-island nations in the low-latitude to midlatitude Pacific (e.g., Micronesia) and Indian (e.g., Chagos islands) Oceans due to their susceptibility to sea level rises from ice mass loss from glaciers and both ice sheets (6) in combination with dynamical sea level changes (Fig. S1). These islands are often fronted by live reef and mangrove systems, which are particularly sensitive to changing environmental conditions, especially rapidly rising sea levels that exacerbate the damaging effects of the frequent tropical cyclone storm surges (3).

Almost all of the 136 largest coastal cities (4) have projected median sea level rises of at least 0.9 m by 2100, with 95th percentile upper limits close to 2 m for the megacities of Southeast and South Asia, and large cities along the Atlantic coast of North America (Table 2 and Table S2). Only a small number of cities in northern Europe, including Glasgow, London, and Dublin, have lower median probable rises of around 0.5 m to 0.7 m (Table 2 and Table S2). The gravitational response to ice loss from Greenland and Antarctic ice sheets (12, 14) and isostatic rebound from previous glaciations mean that the only coasts where sea level rises below the global mean are expected are around Greenland and Antarctica, parts of the Arctic, Pacific Alaska, and northern Europe (Fig. 3).

Discussion and Conclusion

Uncertainties in projected sea level rise vary spatially and temporally, although they increase considerably with warming above 2 °C and reach 1.2 m (5 to 95% range) north of 35°S (Fig. S2 F and I) by 2100. Our estimate of the 95th percentile global sea level rise (1.8 m) is 0.6 m higher than the 1.2 m (95th percentile) published previously (9). This is mainly due to differences in defining the contribution from the ice sheets. The Fifth Assessment Report of the Intergovernmental Panel on Climate Change (AR5 IPCC) (6) provides sea level projections spanning a likely range (66%) and with medium confidence only, largely due to difficulties in projecting ice mass loss from the Greenland and Antarctica ice sheets (10, 16). Both the present study and Kopp et al. (9) therefore used a formal expert elicitation (22) to derive uncertainties of the Antarctic contribution. Kopp et al. (9) reduced these ice dynamics estimates to match the IPCC AR5 central estimates (6), although Oppenheimer et al. (23) suggest that, in doing this, the central range may not be internally consistent with the appended tail. In contrast to Kopp et al. (9), we argue that there is no justification for diminishing the tail risk as perceived by experts (10, 16) and allow for the full range of expert uncertainties as estimated by

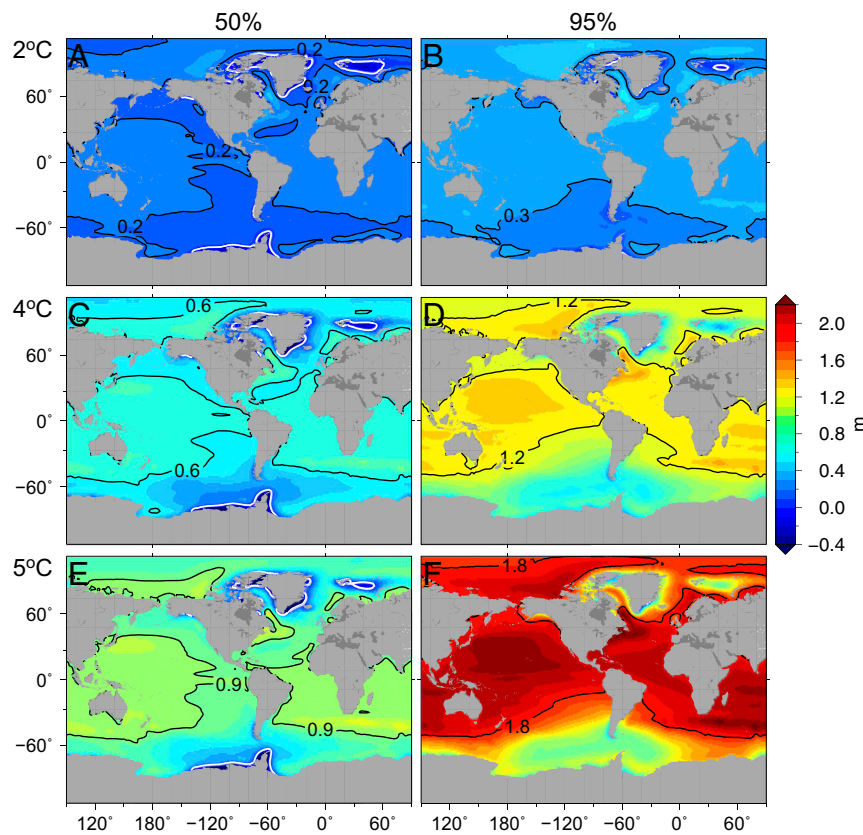


Fig. 2. Regional sea level projections for warming of (A and B) 2 °C (under RCP8.5), (C and D) 4 °C (under RCP8.5), and (E and F) 5 °C (under RCP8.5) relative to 1986–2005. A, C, and E show median projections, and B, D, and F show upper limits (95%). Black contours mark global sea level value, and white contours correspond to zero sea level rise.

Bamber and Aspinall (22). Two recent ice sheet model studies came to different conclusions regarding the plausibility of the high-end tail. Ritz et al. (24) concluded that Antarctic contributions of a meter or more are implausible, whereas DeConto and Pollard (25) find that, not only is this plausible, but it should even be considered likely. The wide uncertainties used in the present study are therefore supported by process models (24, 25). This difference in dealing with the ice dynamics uncertainties especially affects the key finding of this study that, with warming above 2 °C, coastal sea level rises are much larger than global mean sea level rise (Figs. 2, 4, and 5). Fractional variance of the individual sea level rise components varies considerably over time, with Antarctica accounting for 65% at 2 °C and 80% at 4 °C warming (Fig. S3). Despite incorporating observational constraints (24), model uncertainties are likely to remain high until key processes, such as large-scale calving (6, 26, 27), are better understood and parameterized (6, 17). Uncertainties in sea level projections for coastal areas are larger than those for global sea level rise due to the additional mechanisms having regional fingerprints, especially ocean dynamics (Figs. S1–S3). City subsidence potentially introduces large uncertainties in local sea level projections, with up to 3 m by 2100 expected in the case of Jakarta (28).

Many cities, under pressure to expand urban area and housing either because of urban migration or due to rising property prices, are building on land left previously unoccupied because of flood risk. For example, in Guangzhou (China), 6% of the population (4) currently live within 0.5 m of sea level. Guangzhou may be globally the most economically vulnerable city to rising sea levels by the middle of the 21st century, with estimated losses of \$254 million per year under a sea level rise of 0.2 m (4); however, other cities in India, Bangladesh, and Southeast Asia (Table 2 and Table S2) will likely have larger

populations at risk by that date (29, 30). In several coastal cities, current land subsidence exceeds observed sea level rise (15, 28, 31, 32). Economic development in urban areas of megacities drives the growing demand for groundwater, therefore increasing subsidence rates, with 2025 projected (15, 28) sinking of Jakarta (1.8 m), Manila (0.4 m), Ho Chi Minh City (0.2 m), Bangkok (0.19 m), New Orleans (>0.2 m), and the western Netherlands (0.07 m). The costs of local rising sea levels for coastal cities will be much larger than those due to socioeconomic changes, and could amount to US \$ 1 trillion per year in the absence of appropriate adaptation measures (4). Subsidence projected for Jakarta by 2100 varies between 2.3 m and 3.0 m, depending on groundwater management scenario (28). Hence, individual city actions allow for mitigation of, or must provide adaptation to, subsidence; this contrasts with climate-driven sea level rise, which is a global problem that requires global solutions. Without restrictions on groundwater extraction, development of alternative water supplies, and natural and artificial recharge of aquifers, parts of Jakarta, Ho Chi Minh City, Bangkok, and numerous other coastal cities will sink below sea level.

Currently, and despite implementation of climate mitigation measures in several regions (33), global greenhouse gas emissions are following the highest, RCP 8.5, emission trajectory (34, 35). Geoengineering, either by solar radiation management (36) or targeted at preventing sea level rise (37), is being explored as a supplement greenhouse gas mitigation or stop-gap approach to limit some impacts of dangerous warming. However, although the potential exists to reduce global temperatures by, e.g., stratospheric sulfate aerosol injection, there are doubts as to its effectiveness at the quantities needed to reduce radiative forcing from RCP8.5 to, e.g.,

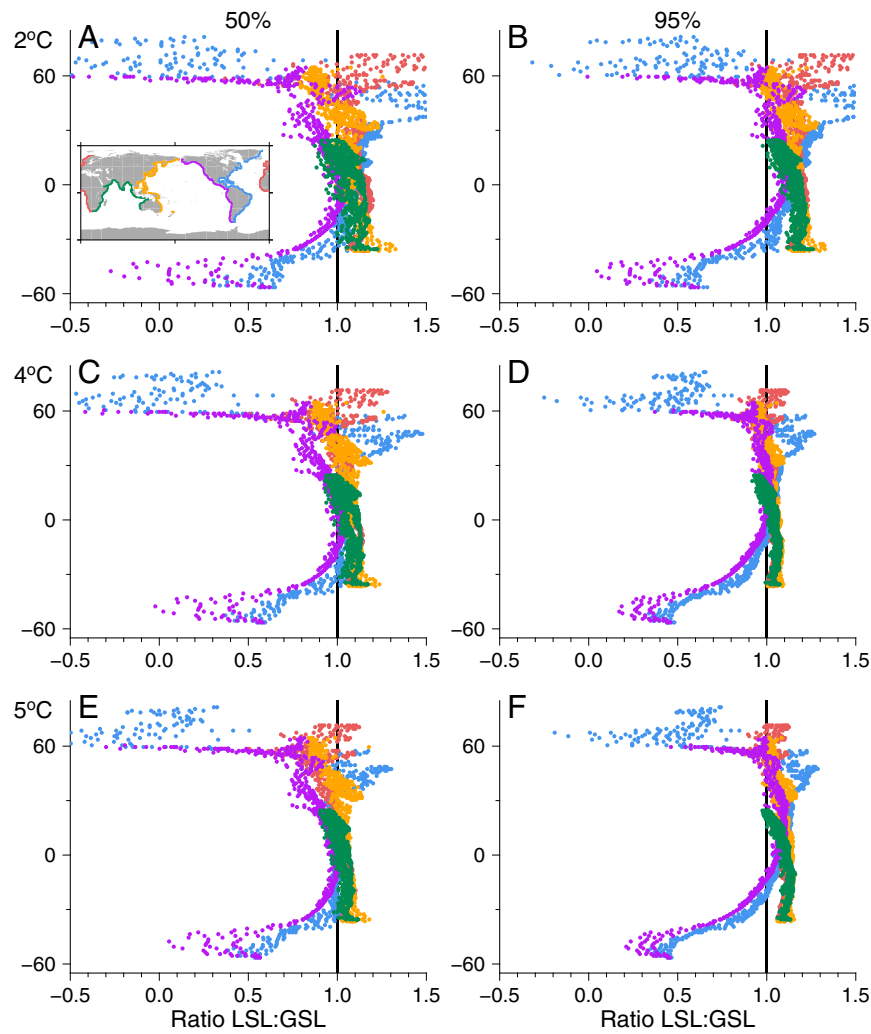


Fig. 3. (A, C, and E) Ratio of projected local (1° grid cells close to coastline) median (50%) sea level rise to global median sea level rise and (B, D, and F) ratio of projected 95% local to 95% global sea level rise with RCP8.5 along global coastlines for warmings of (A and B) 2°C , (C and D) 4°C , and (E and F) 5°C . Colored points show the regional sea level projections for coastlines (color-coded grid points on *Inset map* in A). Vertical black line represents ratio of 1.

RCP4.5 levels (36, 38). Furthermore, the success of geoengineering schemes for combatting sea level rise also depends on preventing warm ocean waters from reaching the undersides of floating ice masses fringing Antarctica; this mechanism depends on complex interactions of surface winds, sea ice, and ocean circulation, and some simulations suggest that aerosol injection may not alter these as desired (39).

After 2040, if warming continues well above 2°C as under the RCP8.5 scenario, global sea level rise will exceed $10\text{ mm}\cdot\text{y}^{-1}$ by 2083. At 4°C warming, more than 80% of coastlines will exceed a median global sea level of 0.6 m. Historically unprecedented changes in sea level rise (Fig. 4) with warming above 2°C will limit time for adaptation in the vast areas of agricultural land, wetlands, beaches, and coastal cities affected. Some low-lying developing countries (e.g., Bangladesh and Vietnam) and small islands will be expected to deal with very high impacts, and associated annual damage and adaptation costs will be several percentage points of gross domestic product (5, 40). Sea level rise of 2 m will lead to the displacement of urban populations: 2.5 million living in low-lying areas of Miami; 2.1 million in Guangzhou; 1.8 million in Mumbai; and more than 1 million each in Osaka, Tokyo, New Orleans, New York, and Ho Chi Minh City (4). The impacts of sea level rise in coastal regions

will not be uniform (Figs. 2 and 4), and the challenge of adapting to extremely rapid sea level rise will affect individuals, communities, countries, and the global population. The next generation or two will face unprecedented challenges to protect coastal United Nations Educational, Scientific and Cultural Organization Cultural World Heritage sites (41) such as Venice, Alexandria, and Qal'at al-Bahrain as well as vulnerable tropical coastal ecosystems.

Materials and Methods

We use a probabilistic approach (10, 16) in which the main sea level components are represented by pdfs to accommodate the considerable uncertainties existing in these components. For regional sea level projections, we follow the approach of Grinsted et al. (10) and combine fingerprints of the main sea level components,

$$\text{RSL} = F(T) + F(G) + F(\text{Gr}) + F(A) + F(\text{LW}) + F(\text{GIA}), \quad [1]$$

where RSL is regional sea level, $F(T)$, $F(G)$, $F(\text{Gr})$, $F(A)$, $F(\text{LW})$ are the fingerprints [$F()$], respectively, of steric sea level changes plus dynamical changes in sea surface height (T); ice loss from glaciers (surface mass balance) (G); ice loss from Greenland (surface mass balance and ice dynamics) (Gr); ice loss from Antarctica ice sheet (surface mass balance and ice dynamics) (A); and land water, including water storage in artificial reservoirs and groundwater mining (LW). To generate regional sea level

Table 2. Probabilistic projections (5%, 50%, and 95% quantiles) of sea level rise (meters) in selected cities with warming of 2 °C, 4 °C, and 5 °C

City	2 °C			4 °C			5 °C		
	5%	50%	95%	5%	50%	95%	5%	50%	95%
Bangkok	0.12	0.19	0.32	0.35	0.59	1.17	0.49	0.87	1.91
Dublin	0.10	0.18	0.31	0.28	0.52	1.12	0.36	0.73	1.79
Glasgow	0.03	0.11	0.25	0.11	0.38	0.97	0.15	0.54	1.58
Guangzhou	0.12	0.21	0.34	0.36	0.62	1.20	0.51	0.91	1.93
Hamburg	0.17	0.27	0.40	0.42	0.69	1.25	0.56	0.95	1.95
Ho Chi Minh	0.12	0.20	0.33	0.37	0.62	1.20	0.50	0.90	1.96
Hong Kong	0.13	0.20	0.32	0.37	0.61	1.18	0.52	0.90	1.90
Jakarta	0.11	0.18	0.30	0.34	0.58	1.12	0.49	0.85	1.80
Kuala Lumpur	0.11	0.18	0.31	0.33	0.58	1.19	0.47	0.86	1.92
Lagos	0.14	0.21	0.34	0.38	0.62	1.20	0.52	0.90	1.92
London	0.12	0.20	0.33	0.30	0.55	1.15	0.38	0.75	1.82
Manila	0.13	0.20	0.34	0.37	0.63	1.22	0.51	0.92	1.99
New Orleans	0.16	0.24	0.37	0.39	0.63	1.27	0.52	0.88	2.01
New York	0.20	0.31	0.46	0.48	0.78	1.43	0.64	1.09	2.24
San Francisco	0.10	0.16	0.30	0.27	0.49	1.15	0.37	0.73	1.87

No corrections for local subsidence rate have been applied.

projections for particular degree (2 °C, 4 °C, and 5 °C) warming, we randomly sample the pdf of each sea level component (Fig. 1 C and E–H). We simultaneously produce fingerprints for each component (excluding GIA, which is a nonclimate related component) by scaling the normalized fingerprint of each component by their associated random samples. We then sum the fingerprints of the sea level components making, in total, 5,000 realizations of sea level. This allows us to create a pdf for each grid point in our map of regional sea level projections associated with 2 °C, 4 °C, and 5 °C warming. To account for the redistribution of ocean mass due to GIA,

we add the time-integrated global field of sea level from the ICE 6G model (13) to the sum of sea level components.

Fig. 1 C and E–H shows the pdfs for each individual component with 2 °C, 4 °C, and 5 °C warming used for calculation of regional sea level patterns. For the $F(T)$ component, we calculate pdfs from the available outputs of 33 climate models (Table S1) in the World Climate Research Program CMIP5 (42). Dynamical changes in sea level (zos; here we give the CMIP5 variable names) and global average steric sea level change (zossga) for time slices 2030–2050 (2 °C) and 2070–2090 (4 °C) warming were used to accommodate the uncertainties in global temperature warmings (Fig. 1A) under RCP8.5. Inverse barometric corrections were made using atmospheric pressure and atmospheric water content to zos. Model drift for historical simulations (1850–2005) and projections (2006–2100) in zossga and zos was corrected using linear regression of the full-length pre-industrial control run from each model experiment and at each grid node independently. The multimodel ensemble means from global average steric sea level change (zossga) and dynamic sea level (zos) for each individual model are shown in Fig. S1 for 2 °C, 4 °C, and 5 °C warmings.

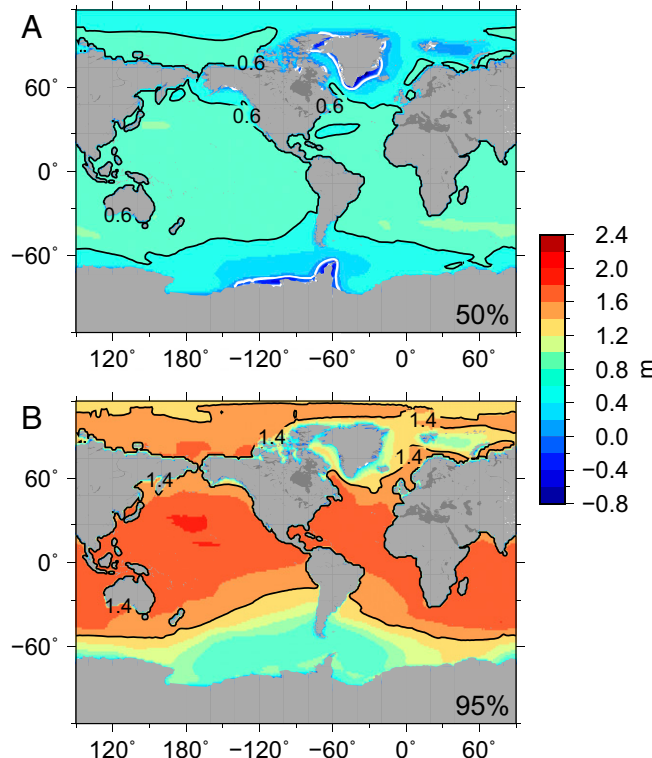


Fig. 4. Increases in regional sea level change under 5 °C warming compared with 2 °C: (A) median increases and (B) increases in the 95th percentile. Black line marks increases of (A) 0.6 m and (B) 1.4 m in global average sea level. White line corresponds to zero sea level rise.

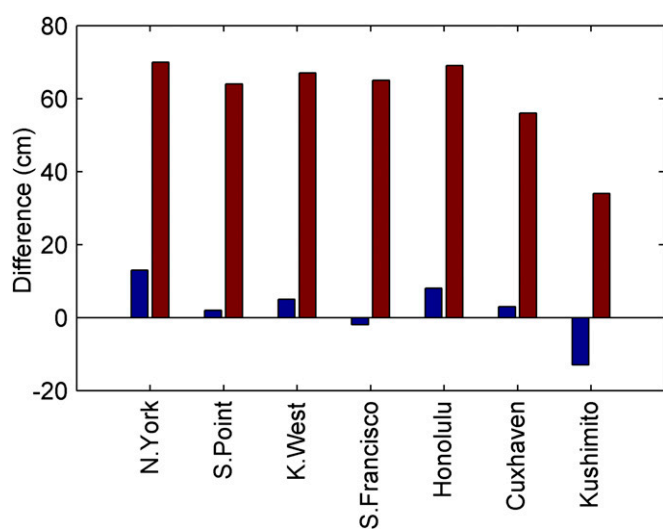


Fig. 5. Difference in sea level projections (centimeters) for median (blue) and 95th percentile (brown) with RCP8.5 scenario at individual locations by 2100 (this study; Table S3) (9). This difference is mainly due to distinction in defining the contribution from the ice sheets, particularly how the expert assessments from ice dynamicists (22) is accounted for.

For other components [$F(G)$, $F(\text{Gr})$, $F(A)$, and $F(\text{LW})$] from Eq. 1, we construct pdfs by using the component pdfs for the year 2100 (16) and assume constant change of rate over the 21st century to construct curves of sea level components, with tests for scaling following the approach of Perrette et al. (43). We fit a pdf to sea level components at 2100 using the forward model of the Burr distribution (44, 45),

$$f(x|\alpha, c, k) = \frac{\frac{k\alpha}{c} \left(\frac{x}{\alpha}\right)^{c-1}}{\left[1 + \left(\frac{x}{\alpha}\right)^c\right]^{k+1}} \quad [2]$$

where α is the scale parameter and c and k are shape parameters ($x; \alpha; c; k > 0$). We search over α , c , and k using the Nelder–Mead simplex method (46) to create a pdf whose distribution minimizes the root-mean-square between modeled and “observed” 5%, 50%, and 95% probabilities for each component

1. Framework Convention on Climate Change (2009) *Action Taken by the Conference of the Parties at Its Fifteenth Session* (United Nations, Geneva), FCCC/CP/2009/11/Add.1.
2. Stern N (2006) *Stern Review on The Economics of Climate Change. Executive Summary* (HM Treasury, London).
3. Woodruff JD, Irish JL, Camargo SJ (2013) Coastal flooding by tropical cyclones and sea-level rise. *Nature* 504(7478):44–52.
4. Hallegatte S, Green C, Nicholls RJ, Corfee-Morlot J (2013) Future flood losses in major coastal cities. *Nat Clim Change* 3:802–806.
5. Intergovernmental Panel on Climate Change (IPCC) (2013) Summary for Policymakers. *Climate Change 2013: The Physical Science Basis. Contribution of Working Group I to the Fifth Assessment Report of the Intergovernmental Panel on Climate Change*, eds Stocker TF, et al. (Cambridge Univ Press, Cambridge, UK).
6. Church JA, et al. (2013) Sea Level Change. *Climate Change 2013: The Physical Science Basis. Contribution of Working Group I to the Fifth Assessment Report of the Intergovernmental Panel on Climate Change*, eds Stocker TF, et al. (Cambridge Univ Press, Cambridge, UK).
7. Schaeffer M, Hare W, Rahmstorf S, Vermeer M (2012) Long-term sea-level rise implied by 1.5°C and 2°C warming levels. *Nat Clim Change* 2:867–870.
8. Slanger ABA, et al. (2014) Projecting twenty-first century regional sea-level changes. *Clim Change* 124(1):317–332.
9. Kopp RE, et al. (2014) Probabilistic 21st and 22nd century sea-level projections at a global network of tide-gauge sites. *Earth's Futur* 2(8):383–406.
10. Grinsted A, Jevrejeva S, Riva R, Dahl-Jensen D (2015) Sea level rise projections for Northern Europe under RCP8.5. *Clim Res* 64(1):15–23.
11. Stammer D, Cazenave A, Ponte RM, Tamisiea ME (2013) Causes for contemporary regional sea level changes. *Annu Rev Mar Sci* 5(1):21–46.
12. Mitrovica JX, Tamisiea ME, Davis JL, Milne GA (2001) Recent mass balance of polar ice sheets inferred from patterns of global sea-level change. *Nature* 409(6823):1026–1029.
13. Peltier WR, Argus DF, Drummond R (2015) Space geodesy constrains ice age terminal deglaciation: The global ICE-6G_C (VM5a) model. *J Geophys Res Solid Earth* 120(1):450–487.
14. Bamber J, Riva R (2010) The sea level fingerprint of recent ice mass fluxes. *Cryosphere* 4(4):621–627.
15. De Lange G, Bux T, Stuurman R, Erkens G (2015) Land subsidence, sea level rise and urban flooding: Coping strategies in coastal cities. *E-proceedings of the 36th IAHR World Congress* (Int Assoc Hydro-environ Eng Res, The Hague). Available at 89.31.100.18/~iahrpapers/90723.pdf. Accessed December 1, 2015.
16. Jevrejeva S, Grinsted A, Moore J (2014) Upper limit for sea level projections by 2100. *Environ Res Lett* 9:104008.
17. Moore JC, Grinsted A, Zwinger T, Jevrejeva S (2015) Semi-empirical and process-based global sea level projections. *Rev Geophys* 53(3):484–522.
18. Pattyn F, et al. (2013) Grounding-line migration in plan-view marine ice-sheet models: results of the ice2sea MISMIP3d intercomparison. *J Glaciol* 59(215):410–422.
19. Wada Y, et al. (2012) Past and future contribution of global groundwater depletion to sea-level rise. *Geophys Res Lett* 39(9):L09402.
20. Christensen OB, et al. (2015) Scalability of regional climate change in Europe for high-end scenarios. *Clim Res* 64(1):25–38.
21. Department of Economic and Social Affairs, Population Division (2014) *World Urbanization Prospects: The 2014 Revision, Highlights* (United Nations, Geneva), ST/ESA/SER.A/352.
22. Bamber JL, Aspinall W (2013) An expert judgement assessment of future sea level rise from the ice sheets. *Nat Clim Change* 3:424–427.
23. Oppenheimer M, Little CM, Cooke RM (2016) Expert judgement and uncertainty quantification for climate change. *Nat Clim Change* 6:445–451.
24. Ritz C, et al. (2015) Potential sea-level rise from Antarctic ice-sheet instability constrained by observations. *Nature* 528(7580):115–118.
25. DeConto RM, Pollard D (2016) Contribution of Antarctica to past and future sea-level rise. *Nature* 531(7596):591–597.
26. Pollard D, DeConto RM, Alley RB (2015) Potential Antarctic Ice Sheet retreat driven by hydrofracturing and ice cliff failure. *Earth Planet Sci Lett* 412:112–121.
27. Åström JA, et al. (2015) Terminii of calving glaciers as self-organized critical systems. *Nat Geosci* 7:874–878.
28. Erkens G, Bux T, Dam R, de Lange G, Lambert J (2015) Sinking coastal cities. *Proc IAHS* 372:189–198.
29. Nicholls RJ, et al. (2008) *Ranking Port Cities with High Exposure and Vulnerability to Climate Extremes: Exposure Estimates* (Org Econ Coop Dev, Paris), Environ Work Pap 1.
30. Hinkel J, et al. (2014) Coastal flood damage and adaptation costs under 21st century sea-level rise. *Proc Natl Acad Sci USA* 111(9):3292–3297.
31. Bux THM, van Ruiten CJM, Erkens G, de Lange G (2015) An integrated assessment framework for land subsidence in delta cities. *Proc IAHS* 372:485–491.
32. Wöppelmann G, Marcos M (2016) Vertical land motion as a key to understanding sea level change and variability. *Rev Geophys* 54(1):64–92.
33. White House (2014) *U.S.-China Joint Announcement on Climate Change and Clean Energy Cooperation 2014* (Off Press Sec, Washington, DC). Available at <https://www.whitehouse.gov/the-press-office/2014/11/11/fact-sheet-us-china-joint-announcement-climate-change-and-clean-energy-c>. Accessed November 3, 2015.
34. Peters GP, et al. (2013) The challenge to keep global warming below 2°C. *Nat Clim Change* 3:4–6.
35. Le Quéré C, et al. (2015) Global carbon budget 2014. *Earth Syst Sci Data* 7(1):47–85.
36. Kravitz B, et al. (2015) The Geoengineering Model Intercomparison Project Phase 6 (GeoMIP6): Simulation design and preliminary results. *Geosci Model Dev* 8(10):3379–3392.
37. Frieler K, Mengel M, Levermann A (2016) Delaying future sea-level rise by storing water in Antarctica. *Earth Syst Dyn* 7(1):203–210.
38. Niemeier U, Timmreck C (2015) What is the limit of stratospheric sulfur climate engineering? *Atmos Chem Phys* 15(7):10939–10969.
39. McCusker KE, Battisti DS, Bitz CM (2015) Inability of stratospheric sulfate aerosol injections to preserve the West Antarctic Ice Sheet. *Geophys Res Lett* 42(12):4989–4997.
40. World Bank (2007) *The Impact of Sea Level Rise on Developing Countries: A Comparative Analysis* (World Bank, Washington, DC), Policy Res Work Pap 4136.
41. Marzeion B, Levermann A (2014) Loss of cultural world heritage and currently inhabited places to sea-level rise. *Environ Res Lett* 9:104008.
42. Taylor K, Stouffer RJ, Meehl GA (2012) An overview of CMIP5 and the experiment design. *Bull Am Meteorol Soc* 93(4):485–498.
43. Perrette M, Landerer F, Riva R, Frieler K, Meinshausen M (2013) A scaling approach to project sea level rise and its uncertainties. *Earth Syst Dyn* 4(1):11–29.
44. Burr IW (1942) Cumulative frequency functions. *Ann Math Stat* 13(2):215–232.
45. Tadikamalla PR (1980) A look at the Burr and related distributions. *Int Stat Rev* 48(3): 337–344.
46. Lagarias JC, Reeds JA, Wright MH, Wright PE (1998) Convergence properties of the Nelder–Mead simplex method in low dimensions. *SIAM J Optim* 9(1):112–147.

at 2° and 4° time slices. Sea level component pdfs at 2100 (16) represent the uncertainties in sea level components with warming of 5 °C.

ACKNOWLEDGMENTS. We thank Y. Wada for data sharing. S.J. and L.P.J. received funding from the European Union’s Seventh Programme for Research, Technological Development and Demonstration under Grant Agreement FP7-ENV-2013-Two-Stage-603396- RISES-AM. R.E.M.R. acknowledges funding from The Netherlands Organisation for Scientific Research through VIDI Grant 864.12.012. J.C.M. was funded by the National Basic Research Program of China (Grant 2015CB953602). A.G. was funded by ERC Advanced Grant 246815 (WATERUNDERTHEICE). L.P.J. is currently funded by the Robertson Foundation (Grant 9907422). We acknowledge the World Climate Research Programme’s Working Group on Coupled Modelling, which is responsible for CMIP, and we thank the climate modeling groups for producing and making available their model outputs.

Supporting Information

Jevrejeva et al. 10.1073/pnas.1605312113

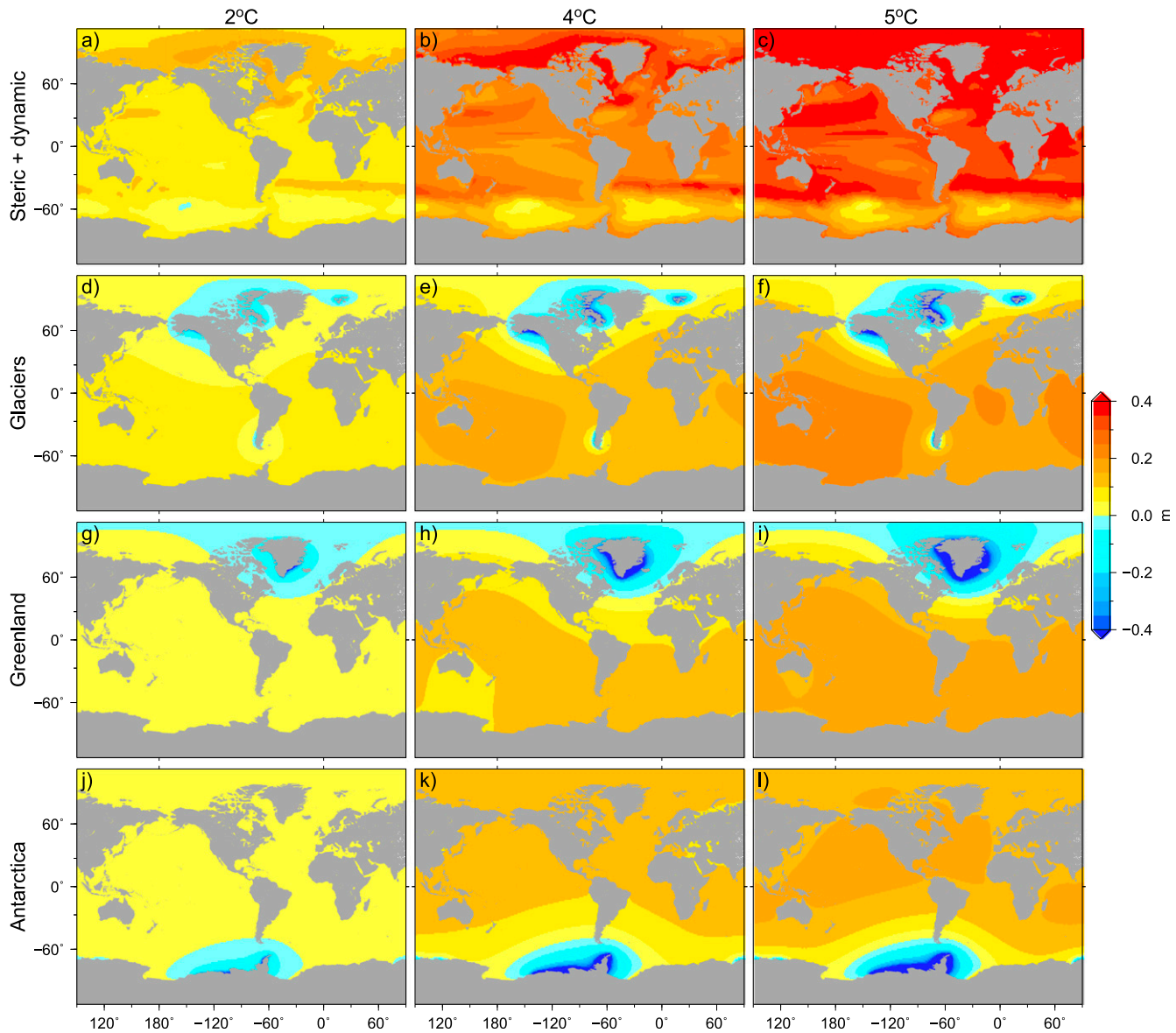


Fig. S1. Projected median (50%) contributions (meters) to regional sea level rise from (A–C) ocean (steric + dynamic), (D–F) glaciers, (G–I) Greenland ice sheet, and (J–L) Antarctica ice sheet with (A, D, G, and J) warming of 2 °C, (B, E, H, and K) 4 °C, and (C, F, I, and L) 5 °C.

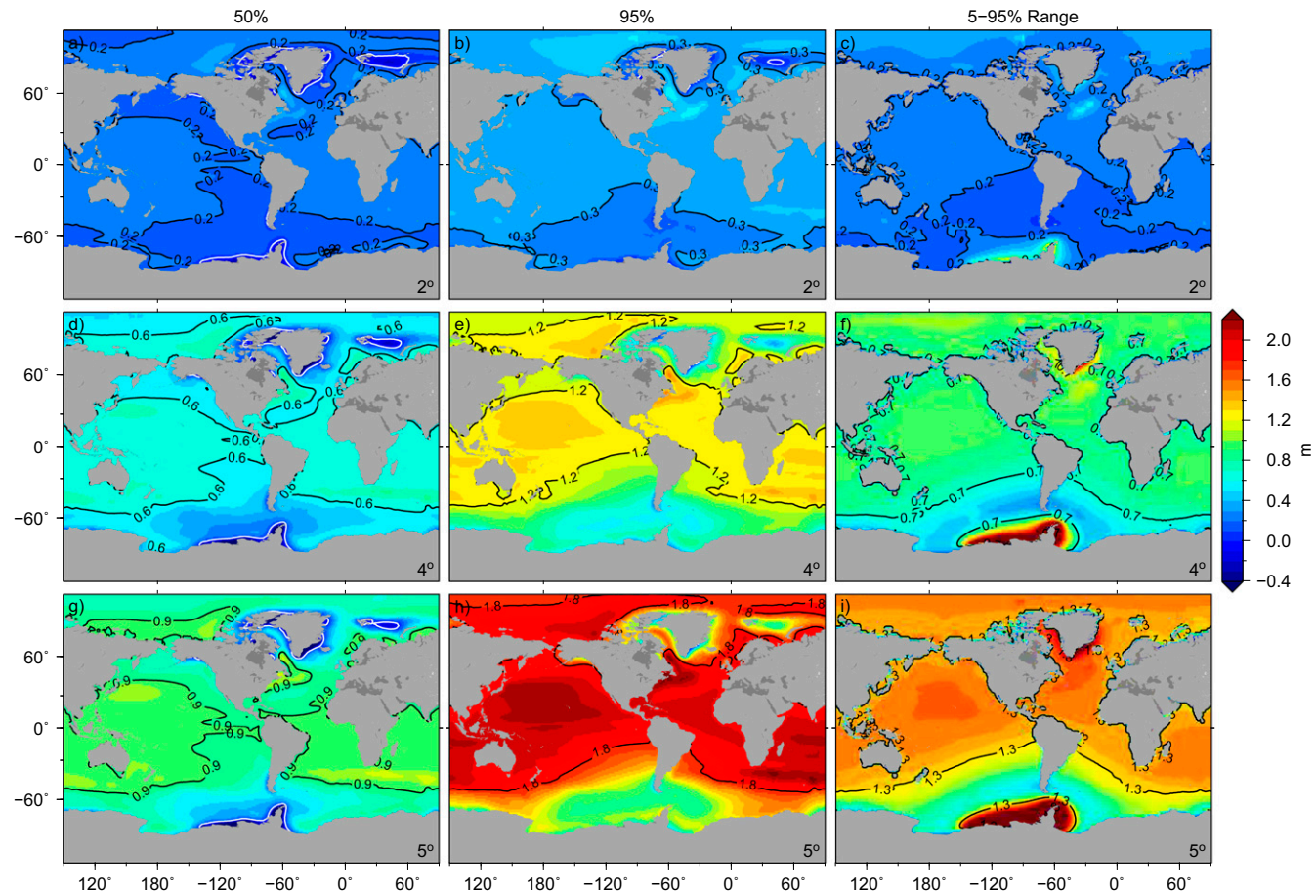


Fig. S2. Regional sea level projections for warming of (A–C) 2 °C (at 2041 under RCP8.5; 2050 under RCP4.5), (D–F) 4 °C (under RCP8.5), and (G–I) 5 °C under RCP8.5 relative to 1986–2005. A, D, and G show median projections, which can be considered the best guess, with (B, E, and H) upper limit projections defined as 95% probability. C, F, and I show the 95 to 5% uncertainty range. Black contours show the global values in each plot: (A) 0.2 m, (B) 0.3 m, (C) 0.2 m, (D) 0.6 m, (E) 1.2 m, (F) 0.7 m, (G) 0.9 m, (H) 1.8 m, and (I) 1.3 m. White contours correspond to zero sea level rise.

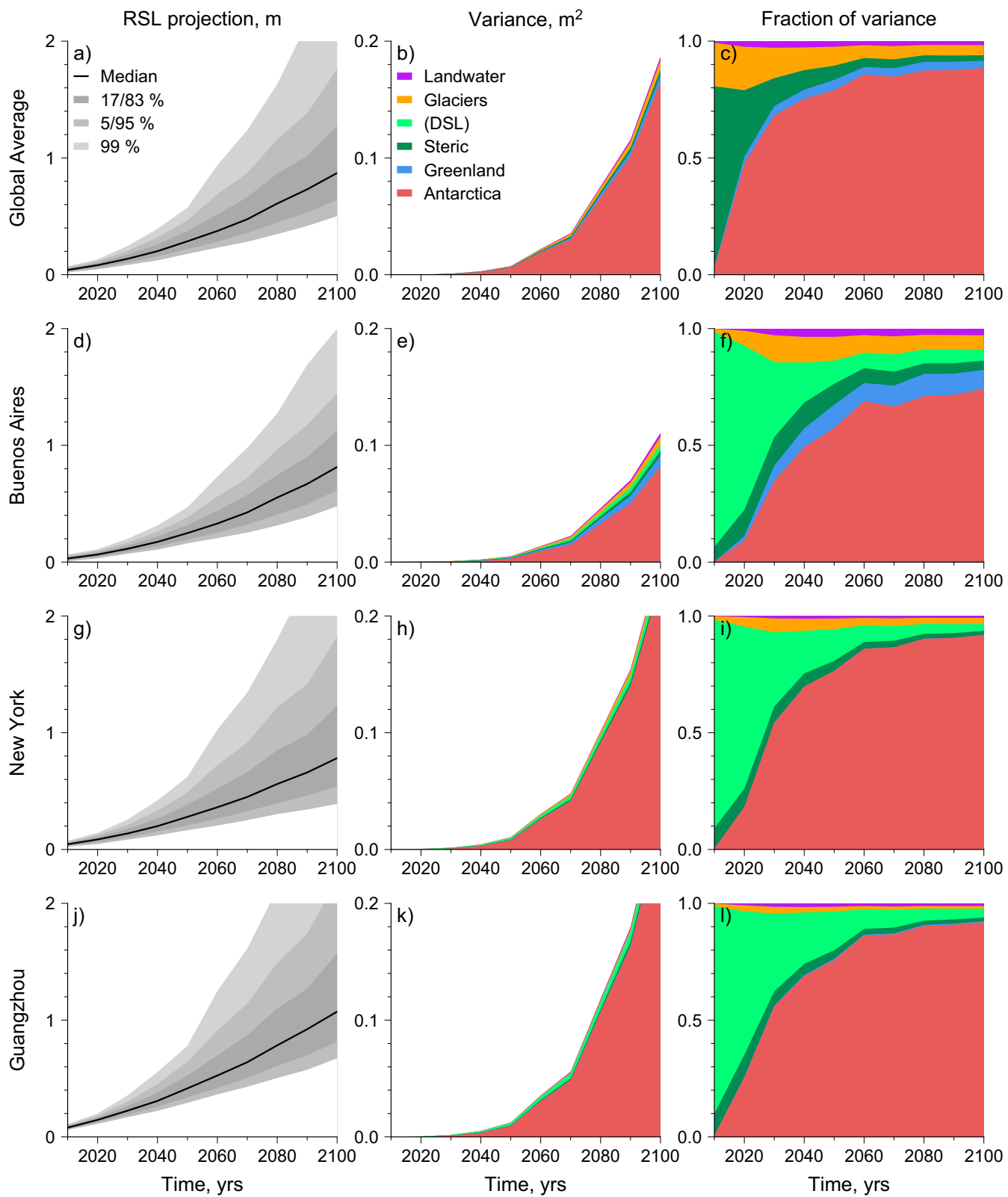


Fig. S3. Probabilistic projections of (A) global sea level rise and (D, G, and J) selected individual locations representing the 5%, 17%, 50%, 83%, 95%, and 99% quantiles, RCP8.5 scenario. (B, E, H, and K) Variance (square meters) in components; colors represent different sources of sea level as in key on B. (C, F, I, and L) Fraction of components' variance in global sea level rise, with colors as in B.

Table S1. List of the models from CMIP5 used in this study for calculation of global average steric sea level change and dynamic sea levels

Model	Number of realizations for RCP8.5
bcc-csm1-1	1
bcc-csm1-1-m	1
CanESM2	5
CMCC-CESM	1
CMCC-CM	1
CMCC-CMS	1
CNRM-CM5	5
ACCESS1-0	1
ACCESS1-3	1
CSIRO-MK3-6-0	10
EC-EARTH	12
inmcm4	1
IPSL-CM5A-LR	4
IPSL-CM5A-MR	1
IPSL-CM5B-LR	1
FGOALS-g2	1
MIROC5	3
MIROC-ESM	1
MIROC-ESM-CHEM	1
HadGEM2-CC	3
HadGEM2-ES	4
MPI-ESM-LR	3
MPI-ESM-MR	1
MRI-CGCM3	1
GISS-E2-R	3
CCSM4	6
NorESM1-M	1
NorESM1-ME	1
GFDL-ESM2G	1
GFDL-ESM2M	1
CESM1-BGC	1
CESM1-CAM5	2
CESM1-WACCM	3
Total models	33
Total realizations	83

Table S2. Probabilistic projections (5%, 50%, and 95% quantiles) of sea level rise (meters) in 136 coastal cities (4) with warming of 2 °C, 4 °C, and 5 °C

City	Longitude	Latitude	2 °C			4 °C			5 °C		
			0.05	0.50	0.95	0.05	0.50	0.95	0.05	0.50	0.95
Accra	359.80	5.55	0.15	0.22	0.35	0.39	0.64	1.24	0.52	0.92	1.97
Adelaide	138.60	-34.93	0.12	0.21	0.34	0.33	0.60	1.18	0.43	0.87	1.90
Amsterdam	4.90	52.37	0.14	0.21	0.34	0.34	0.59	1.16	0.44	0.81	1.82
Auckland	174.76	-36.85	0.15	0.23	0.36	0.41	0.68	1.23	0.56	0.97	1.94
Baltimore	283.39	39.29	0.23	0.33	0.48	0.52	0.80	1.44	0.67	1.08	2.22
Bangkok	100.50	13.76	0.12	0.19	0.32	0.35	0.59	1.17	0.49	0.87	1.91
Barranquilla	285.19	11.00	0.15	0.23	0.36	0.38	0.63	1.24	0.50	0.89	1.98
Belém	311.51	-1.46	0.14	0.21	0.34	0.37	0.62	1.19	0.49	0.89	1.90
Boston	288.94	42.36	0.18	0.29	0.46	0.43	0.73	1.38	0.58	1.01	2.12
Brisbane	153.02	-27.47	0.15	0.22	0.35	0.40	0.65	1.25	0.53	0.94	1.98
Buenos Aires	301.62	-34.60	0.11	0.17	0.26	0.33	0.54	0.94	0.46	0.81	1.49
Calcutta	88.36	22.57	0.10	0.18	0.31	0.29	0.56	1.13	0.40	0.81	1.77
Cape Town	18.42	-33.92	0.14	0.21	0.34	0.39	0.64	1.21	0.51	0.92	1.92
Casablanca	352.41	33.57	0.14	0.20	0.33	0.35	0.58	1.17	0.46	0.82	1.86
Chennai	80.27	13.08	0.11	0.18	0.31	0.33	0.57	1.14	0.46	0.84	1.85
Chittagong	91.80	22.37	0.10	0.18	0.31	0.29	0.56	1.13	0.40	0.81	1.77
Cochin	76.27	9.93	0.13	0.20	0.34	0.37	0.62	1.22	0.52	0.90	1.95
Conakry	346.29	9.51	0.14	0.21	0.34	0.37	0.62	1.22	0.49	0.88	1.95
Copenhagen	12.57	55.68	0.16	0.26	0.40	0.42	0.70	1.27	0.55	0.96	1.93
Dakar	342.63	14.76	0.15	0.22	0.35	0.39	0.64	1.25	0.51	0.92	1.99
Dalian	121.61	38.91	0.12	0.20	0.32	0.35	0.61	1.17	0.50	0.88	1.85
Dar-es-Salaam	39.28	-6.80	0.15	0.22	0.34	0.40	0.64	1.22	0.53	0.91	1.94
Davao	125.46	7.19	0.14	0.21	0.35	0.38	0.64	1.26	0.52	0.94	2.05
Dhaka	90.41	23.81	0.10	0.18	0.30	0.29	0.56	1.12	0.40	0.82	1.76
Douala	9.70	4.05	0.15	0.22	0.35	0.40	0.65	1.22	0.53	0.92	1.94
Dubai	55.27	25.20	0.13	0.20	0.32	0.36	0.60	1.15	0.50	0.87	1.82
Dublin	353.74	53.35	0.10	0.18	0.31	0.28	0.52	1.12	0.36	0.73	1.79
Durban	31.02	-29.86	0.14	0.22	0.35	0.39	0.64	1.24	0.53	0.93	1.95
Fortaleza	321.47	-3.73	0.15	0.21	0.34	0.38	0.62	1.21	0.51	0.90	1.91
Fukuoka-Kitakyushu	130.88	33.88	0.13	0.21	0.34	0.38	0.64	1.21	0.53	0.93	1.95
Fuzhou Fujian	119.30	26.07	0.12	0.20	0.34	0.35	0.61	1.19	0.49	0.90	1.92
Glasgow	355.75	55.86	0.03	0.11	0.25	0.11	0.38	0.97	0.15	0.54	1.58
Grande Vitória	319.70	-20.30	0.13	0.20	0.32	0.37	0.61	1.13	0.50	0.89	1.80
Guangzhou Guangdong	113.26	23.13	0.12	0.21	0.34	0.36	0.62	1.20	0.51	0.91	1.93
Guayaquil	280.08	-2.17	0.13	0.20	0.32	0.36	0.60	1.18	0.49	0.88	1.88
Hai Phòn	106.69	20.84	0.13	0.20	0.32	0.38	0.61	1.16	0.52	0.89	1.87
Hamburg	9.99	53.55	0.17	0.27	0.40	0.42	0.69	1.25	0.56	0.95	1.95
Hangzhou	120.16	30.27	0.12	0.19	0.31	0.35	0.59	1.16	0.49	0.87	1.87
Havana	277.73	23.16	0.14	0.22	0.36	0.36	0.61	1.26	0.47	0.87	2.03
Hiroshima	132.46	34.39	0.12	0.20	0.32	0.37	0.61	1.19	0.51	0.90	1.92
Ho Chi Minh City	106.63	10.82	0.12	0.20	0.33	0.37	0.62	1.20	0.50	0.90	1.96
Hong Kong	114.17	22.29	0.13	0.20	0.32	0.37	0.61	1.18	0.52	0.90	1.90
Houston	264.63	29.76	0.15	0.22	0.36	0.35	0.60	1.24	0.46	0.85	1.97
Inchon	126.71	37.46	0.12	0.19	0.31	0.35	0.59	1.15	0.50	0.87	1.86
Izmir	27.14	38.42	0.11	0.18	0.30	0.34	0.58	1.12	0.48	0.85	1.79
Jakarta	27.14	38.42	0.11	0.18	0.30	0.34	0.58	1.12	0.48	0.85	1.80
Jiddah	39.17	21.54	0.13	0.21	0.33	0.36	0.61	1.17	0.50	0.89	1.85
Karachi	67.01	24.86	0.10	0.18	0.30	0.28	0.56	1.12	0.39	0.82	1.76
Khulna	89.55	22.82	0.10	0.18	0.31	0.29	0.56	1.13	0.40	0.81	1.77
Kuala Lumpur	101.69	3.14	0.11	0.18	0.31	0.33	0.58	1.19	0.47	0.86	1.92
Kuwait City	47.98	29.38	0.11	0.19	0.31	0.35	0.59	1.15	0.49	0.87	1.87
Lagos	3.38	6.52	0.14	0.21	0.34	0.38	0.62	1.20	0.52	0.90	1.92
Lima	282.96	-12.05	0.13	0.19	0.31	0.36	0.58	1.11	0.50	0.86	1.76
Lisbon	350.86	38.72	0.13	0.20	0.33	0.34	0.58	1.18	0.45	0.81	1.88
Lomé	1.22	6.13	0.16	0.23	0.35	0.40	0.64	1.23	0.53	0.92	1.94
London	359.87	51.51	0.12	0.20	0.33	0.30	0.55	1.15	0.38	0.75	1.82
Los Angeles	241.76	34.05	0.09	0.16	0.29	0.26	0.49	1.15	0.37	0.71	1.88
Luanda	13.23	-8.84	0.16	0.23	0.36	0.41	0.65	1.24	0.54	0.94	1.96
Maceió	324.29	-9.65	0.14	0.21	0.34	0.37	0.61	1.19	0.50	0.89	1.88
Manila	120.98	14.60	0.13	0.20	0.34	0.37	0.63	1.22	0.51	0.92	1.99
Maputo	32.58	-25.97	0.15	0.22	0.35	0.40	0.65	1.25	0.53	0.94	1.96

Table S2. Cont.

City	Longitude	Latitude	2 °C			4 °C			5 °C		
			0.05	0.50	0.95	0.05	0.50	0.95	0.05	0.50	0.95
Maracaibo	288.37	10.63	0.16	0.23	0.37	0.40	0.64	1.25	0.52	0.91	1.99
Melbourne	144.96	-37.81	0.12	0.19	0.32	0.32	0.58	1.14	0.43	0.84	1.84
Miami	279.81	25.76	0.15	0.22	0.37	0.37	0.61	1.26	0.48	0.86	1.99
Mogadishu	45.35	2.03	0.15	0.23	0.35	0.41	0.67	1.27	0.55	0.95	1.99
Montevideo	303.84	-34.90	0.11	0.17	0.26	0.33	0.54	0.94	0.46	0.81	1.49
Montréal	286.43	45.50	0.23	0.33	0.48	0.51	0.82	1.46	0.67	1.11	2.24
Mumbai	72.88	19.08	0.10	0.19	0.31	0.29	0.57	1.15	0.41	0.83	1.79
N'ampopo	125.32	38.75	0.12	0.19	0.31	0.35	0.58	1.12	0.49	0.85	1.82
Nagoya	136.91	35.18	0.14	0.22	0.36	0.39	0.66	1.27	0.55	0.97	2.02
Natal	324.80	-5.78	0.15	0.21	0.34	0.38	0.63	1.22	0.50	0.91	1.93
New Orleans	269.93	29.95	0.16	0.24	0.37	0.39	0.63	1.27	0.52	0.88	2.01
New York	285.99	40.71	0.20	0.31	0.46	0.48	0.78	1.43	0.64	1.09	2.24
Ningbo	121.54	29.87	0.11	0.19	0.31	0.35	0.59	1.15	0.49	0.87	1.87
Odessa	30.72	46.48	0.10	0.20	0.33	0.31	0.60	1.18	0.45	0.87	1.89
Osaka-Kobe	135.50	34.69	0.12	0.20	0.33	0.35	0.60	1.19	0.50	0.90	1.95
Palembang	104.78	-2.98	0.13	0.21	0.34	0.39	0.64	1.26	0.53	0.94	2.03
Panama City	280.48	8.98	0.12	0.19	0.33	0.34	0.59	1.20	0.47	0.86	1.93
Perth	115.86	-31.95	0.12	0.20	0.34	0.35	0.61	1.21	0.48	0.88	1.93
Philadelphia	284.83	39.95	0.23	0.33	0.48	0.52	0.80	1.44	0.67	1.08	2.22
Port-au-Prince	287.67	18.53	0.13	0.20	0.34	0.34	0.60	1.24	0.46	0.87	1.98
Portland	237.32	45.52	0.10	0.17	0.30	0.26	0.49	1.12	0.35	0.70	1.79
Porto	351.37	41.16	0.13	0.20	0.33	0.34	0.57	1.18	0.44	0.79	1.86
Porto Alegre	308.78	-30.03	0.13	0.19	0.29	0.36	0.57	1.00	0.49	0.83	1.58
Providence	288.59	41.82	0.19	0.30	0.46	0.46	0.75	1.41	0.61	1.03	2.16
Pusan	129.08	35.18	0.12	0.21	0.34	0.36	0.63	1.21	0.51	0.91	1.93
Qingdao	120.38	36.07	0.11	0.21	0.35	0.34	0.64	1.22	0.51	0.94	1.92
Rabat	353.15	33.97	0.14	0.20	0.33	0.35	0.58	1.17	0.46	0.82	1.86
Rangoon	96.15	16.78	0.12	0.20	0.32	0.34	0.59	1.16	0.47	0.85	1.86
Recife	325.12	-8.06	0.14	0.21	0.33	0.37	0.61	1.18	0.49	0.88	1.87
Rio de Janeiro	316.83	-22.91	0.13	0.20	0.31	0.37	0.58	1.09	0.49	0.85	1.72
Rotterdam	4.48	51.92	0.14	0.23	0.37	0.35	0.62	1.19	0.45	0.85	1.87
Salvador	270.78	13.69	0.12	0.19	0.32	0.34	0.58	1.21	0.46	0.85	1.95
San Diego	242.84	32.72	0.09	0.15	0.29	0.25	0.48	1.14	0.35	0.70	1.84
San Francisco	237.58	37.77	0.10	0.16	0.30	0.27	0.49	1.15	0.37	0.73	1.87
San Jose	238.11	37.34	0.10	0.16	0.30	0.27	0.49	1.15	0.37	0.71	1.86
San Juan	293.89	18.47	0.13	0.21	0.35	0.35	0.60	1.24	0.47	0.87	2.01
Santo Domingo	290.05	18.47	0.14	0.21	0.35	0.36	0.61	1.25	0.49	0.89	2.03
Santos	313.67	-23.97	0.13	0.20	0.31	0.37	0.61	1.10	0.49	0.88	1.73
Sapporo	141.35	43.06	0.11	0.21	0.35	0.35	0.64	1.23	0.49	0.92	1.96
Seattle	237.67	47.61	0.11	0.18	0.32	0.27	0.51	1.14	0.36	0.72	1.82
Shanghai	121.47	31.23	0.12	0.19	0.31	0.35	0.59	1.16	0.49	0.87	1.87
Shenzhen	114.06	22.54	0.13	0.20	0.32	0.37	0.61	1.18	0.52	0.90	1.90
Singapore	103.82	1.35	0.13	0.20	0.34	0.37	0.62	1.23	0.52	0.92	2.00
Surabaya	112.75	-7.26	0.13	0.21	0.35	0.38	0.63	1.26	0.52	0.93	2.03
Surat	72.83	21.17	0.10	0.19	0.31	0.30	0.57	1.15	0.41	0.83	1.79
Sydney	151.21	-33.87	0.16	0.23	0.36	0.41	0.66	1.25	0.55	0.96	1.97
Taipei	121.57	25.03	0.13	0.21	0.34	0.38	0.64	1.23	0.53	0.93	1.97
Tampa	277.36	27.77	0.17	0.25	0.39	0.41	0.65	1.29	0.53	0.90	2.04
Tianjin	117.20	39.08	0.11	0.18	0.30	0.34	0.56	1.11	0.48	0.84	1.76
Tokyo	139.69	35.69	0.14	0.22	0.36	0.39	0.66	1.27	0.55	0.97	2.02
Ujung Pandang	119.43	-5.15	0.14	0.22	0.35	0.39	0.65	1.28	0.54	0.95	2.05
Ulsan	129.31	35.54	0.12	0.21	0.34	0.36	0.63	1.21	0.51	0.91	1.93
Vancouver	237.34	45.64	0.10	0.17	0.30	0.26	0.49	1.12	0.35	0.70	1.79
Virginia Beach	284.02	36.85	0.20	0.29	0.44	0.48	0.75	1.39	0.63	1.03	2.17
Visakhapatnam	83.22	17.69	0.11	0.18	0.30	0.32	0.56	1.13	0.45	0.84	1.81
Washington, DC	282.96	38.91	0.23	0.31	0.46	0.50	0.77	1.41	0.66	1.05	2.18
Wenzhou	120.70	27.99	0.12	0.19	0.32	0.36	0.60	1.17	0.51	0.89	1.89
Xiamen	118.09	24.48	0.12	0.21	0.35	0.38	0.65	1.23	0.53	0.94	1.95
Yantai	121.45	37.46	0.11	0.20	0.33	0.35	0.63	1.19	0.51	0.92	1.88
Zhanjiang	110.36	21.27	0.13	0.20	0.33	0.37	0.61	1.18	0.52	0.90	1.90

No corrections for local subsidence rate have been applied; GIA vertical land movement corrections (13) have been applied. Cities located in the Baltic and Mediterranean Seas (e.g., Stockholm, Athens, Barcelona) are not included in this table due to limitation of CMIP5 models to simulate dynamic sea level changes in semienclosed seas.

Table S3. Comparison of sea level rise components (centimeters) and total sea level rise for 5%, 50%, and 95% for the RCP8.5 scenario in individual locations at 2100 from Kopp et al. (9) and this study

Location and components	Kopp et al. (9)			This study			Difference, this study – Kopp et al. (9)		
	5%	50%	95%	5%	50%	95%	5%	50%	95%
New York									
GIC	9	14	19	2	11	20	-7	-3	1
GIS	2	6	17	3	5	12	1	-1	-5
AIS	-12	4	38	-8	18	129	4	14	91
Oce	5	51	98	14	49	82	9	-2	-16
LWS	2	5	8	-4	4	15	-6	-1	7
GIA/Tect	12	13	15	17	17	17	5	4	2
Total	44	96	154	64	109	224	20	13	70
Sewell's Point									
GIC	9	15	21	2	12	21	-7	-3	0
GIS	3	8	22	4	6	14	1	-2	-8
AIS	-12	4	38	-8	18	129	4	14	91
Oce	7	46	85	18	46	73	11	0	-12
LWS	2	5	8	-4	4	15	-6	-1	7
GIA/Tect	22	25	27	17	17	17	-5	-8	-10
Total	59	105	158	67	107	220	8	2	62
Key West									
GIC	11	18	24	2	15	26	-9	-3	2
GIS	4	12	32	7	12	26	3	0	-6
AIS	-13	4	39	-8	18	129	5	14	90
Oce	10	39	68	9	33	56	-1	-6	-12
LWS	2	5	8	-4	4	15	-6	-1	7
GIA/Tect	1	5	8	3	3	3	2	-2	-5
Total	46	84	134	49	89	201	3	5	67
Galveston									
GIC	10	16	23	2	11	19	-8	-5	-4
GIS	4	11	31	6	11	25	2	0	-7
AIS	-12	4	38	-8	18	126	4	14	88
Oce	7	38	70	7	35	61	1	-3	-8
LWS	2	5	8	-3	4	12	-5	-1	4
GIA/Tect	43	46	48	5	5	5	-38	-41	-43
Total	83	123	173	48	87	198	-35	-36	25
San Francisco									
GIC	9	15	21	0	0	0	-9	-15	-21
GIS	5	12	35	7	13	28	2	1	-7
AIS	-13	4	39	-9	18	131	4	14	92
Oce	16	37	60	14	33	50	-2	-4	-10
LWS	2	5	8	-1	1	2	-3	-4	-6
GIA/Tect	-2	-1	1	5	5	5	7	6	4
Total	43	75	122	37	73	187	-6	-2	65
Juneau									
GIC	0	3	5	-17	-10	-1	-17	-13	-6
GIS	3	8	23	6	11	25	3	3	2
AIS	-12	4	37	-8	18	129	4	14	92
Oce	20	36	53	13	32	49	-7	-4	-4
LWS	2	5	8	-3	3	12	-5	-2	4
GIA/Tect*	-153	-149	-145	13	13	13	166	162	158
Total	-118	-92	-52	34	72	184	152	164	236
Honolulu									
GIC	12	20	27	3	17	29	-10	-3	2
GIS	6	17	47	10	17	38	4	0	-9
AIS	-14	5	41	-9	19	135	5	14	94
Oce	14	40	66	14	33	51	0	-7	-14
LWS	2	5	8	-4	5	17	-6	0	9
GIA/Tect	-5	-2	1	-1	-1	-1	4	1	-2
Total	48	87	141	53	95	210	5	8	69

Table S3. Cont.

Location and components	Kopp et al. (9)			This study			Difference, this study – Kopp et al. (9)		
	5%	50%	95%	5%	50%	95%	5%	50%	95%
Cuxhaven									
GIC	5	8	12	2	16	28	-3	8	16
GIS	1	2	7	1	1	2	0	-1	-5
AIS	-12	4	36	-7	16	115	5	12	79
Oce	16	51	85	14	41	68	-2	-10	-17
LWS	2	5	8	-2	3	10	-4	-2	2
GIA/Tect	9	10	11	3	3	3	-6	-7	-8
Total	41	81	128	44	84	184	3	3	56
Kushimoto									
GIC	10	18	26	3	19	33	-7	1	7
GIS	6	17	47	10	17	37	4	0	-10
AIS	-13	3	38	-8	16	118	5	13	80
Oce	14	33	73	16	34	51	2	1	-21
LWS	2	5	8	-3	3	12	-5	-2	4
GIA/Tect	8	15	21	-4	-4	-4	-12	-19	-25
Total	63	104	159	52	91	193	-11	-13	34

Sea level components are as follows: AIS, Antarctica ice sheet; GIA/Tect, vertical land movement (note that, in this study, we do no estimate future changes in tectonics, only GIA; we show results for Juneau, but we do not discuss the difference in GIA/Tect in this study); GIC, glaciers; GIS, Greenland ice sheet; LWS, land water storage; Oce, ocean component represented as combination of changes in dynamic sea level and global average static sea level change [as in Kopp et al. (9)]; Total, total sea level rise in individual locations. Note that projections for Stockholm are not included in this table due to limitation of CMIP5 models to simulate dynamic sea level changes in semienclosed seas.